Operation of photonic crystal membrane lasers above room temperature

Po-Tsung Lee,[a] J. R. Cao, Sang-Jun Choi, Zhi-Jian Wei, John D. O'Brien, and P. Daniel Dapkus
Department of Electrical Engineering-Electrophysics, University of Southern California, Los Angeles, California 90089

(Received 25 July 2002; accepted 9 September 2002)

Operation of photonic crystal lasers for substrate temperatures as high as 50 °C is reported. The temperature dependence of the lasing wavelength and the threshold pump power is also investigated. The characteristic temperature T_0 is 37.7 K. © *2002 American Institute of Physics.*
[DOI: 10.1063/1.1517409]

As a promising source for optical communication systems and integrated photonic circuits, the research on two-dimensional (2D) photonic crystal defect lasers has been attracting increasing attention. Single-defect photonic crystal lasers were first demonstrated in pulsed mode at low temperatures.[1] Room-temperature pulsed operation has since been demonstrated in lasers with larger mode volumes,[2–5] and continuous wave room-temperature operation has been reported in a photonic crystal laser with a fusion bonded substrate that had a layer that was subsequently converted to Al_xO_y.[6] Here, we present the experimental results of pulsed operation of optically pumped photonic crystal lasers above room temperature and characterize the thermal behavior of these lasers.

The resonant cavity is formed by removing 19 air holes from a 2D triangular lattice photonic crystal patterned into a semiconductor membrane, which consists of four 10 nm compressively strained InGaAsP quantum wells as the gain media. The laser structure is fabricated by perforating holes through the 224 nm thick membrane by a series of dry etching and wet chemical etching steps.[7] Figure 1 shows a scanning electron micrograph of the oblique view of a column of laser structures with a V-shaped undercut groove.

The fabricated sample is mounted on a piece of copper, which is fixed onto a Peltier thermal electric cooler (TEC) with a heat sink attached. The assembly is then mounted on an $X-Y-Z$ stage. A 10 kΩ thermistor is used to monitor the temperature of the sample. The temperature is controlled by a temperature controller, which has a stability of ±0.004 °C. The membrane defect cavity is optically pumped by an 865 nm top-emitting vertical-cavity surface-emitting laser (VCSEL) at normal incidence. A pump spot size of approximately 4.5 μm is achieved using a long working distance 100× objective lens. A multimode fiber is used to collect the light output from the defect laser and is connected to an optical spectrum analyzer for characterization.

The spontaneous emission spectrum of an unpatterned area (without air holes and undercut structure) shows a broad spectral emission peaked at 1.55 μm with a full width at half maximum of 200 nm after the device fabrication process. When the pump beam is moved to and focused onto the defect cavity, we can expect that the temperature of the defect cavity will be higher due to low thermal conductivity of the air region below the membrane. As a result, the gain spectrum shifts to longer wavelength and so does the lasing wavelength.

To predict the temperature of the defect cavity under optical pumping, a heat transfer analysis using finite element method is performed. Here, we simulate heat conduction of the photonic crystal defect laser membrane structure, and heat convection and radiation are considered as the boundary conditions at the semiconductor/air interfaces. Four-node tetrahedral elements are used to mesh the structure. Temperature-dependent material properties such as density, specific heat, and thermal conductivity are used. The ambient temperature of the structure is set at 300 K and heat source is applied from the top of the defect region. We considered a single-defect cavity with five periods of the photonic crystal lattice on each side of the cavity in this calculation. The smaller resonant cavity is considered to reduce the size of the calculation and is expected to provide an upper bound on the temperature in the larger cavities. We assume the pump spot size is approximately 3.5 μm in diameter and the pump power is 7 mW with 4% duty cycle. A wide range of pump conditions have been explored experimentally. This simulation condition is chosen to illustrate the expected effects of the optical pump on the membrane temperature. Steady-state analysis is performed and only one-sixth of the whole structure is analyzed due to the six-fold symmetry of the geometry. A plot of the simulation result showing the mesh of the whole structure and the temperature distribution is in Fig. 2. The $x-y$ plane is the top surface of the 2D photonic crystal

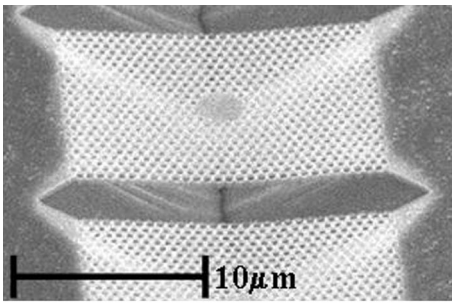

FIG. 1. Oblique view of a fabricated suspended membrane structure. The thickness of the slab waveguide is 224 nm with perforated air holes forming a 2D triangular lattice photonic crystal in plane.

[a]Electronic mail: potsung@usc.edu

Report Documentation Page

Form Approved
OMB No. 0704-0188

1. REPORT DATE	2. REPORT TYPE	3. DATES COVERED
01 JUN 2005	**N/A**	**-**

4. TITLE AND SUBTITLE	5a. CONTRACT NUMBER
Operation of Photonic Crystal Membrane Lasers above room temperature	5b. GRANT NUMBER
	5c. PROGRAM ELEMENT NUMBER
6. AUTHOR(S)	5d. PROJECT NUMBER
	5e. TASK NUMBER
	5f. WORK UNIT NUMBER
7. PERFORMING ORGANIZATION NAME(S) AND ADDRESS(ES) **Department of Electrical Engineering and Electrophysics, University of Southern California, Los Angeles, California 90089**	8. PERFORMING ORGANIZATION REPORT NUMBER
9. SPONSORING/MONITORING AGENCY NAME(S) AND ADDRESS(ES)	10. SPONSOR/MONITOR'S ACRONYM(S)
	11. SPONSOR/MONITOR'S REPORT NUMBER(S)

12. DISTRIBUTION/AVAILABILITY STATEMENT
Approved for public release, distribution unlimited

13. SUPPLEMENTARY NOTES
See also ADM001923.

14. ABSTRACT

15. SUBJECT TERMS

16. SECURITY CLASSIFICATION OF:			17. LIMITATION OF ABSTRACT	18. NUMBER OF PAGES	19a. NAME OF RESPONSIBLE PERSON
a. REPORT	b. ABSTRACT	c. THIS PAGE			
unclassified	**unclassified**	**unclassified**	**UU**	**3**	

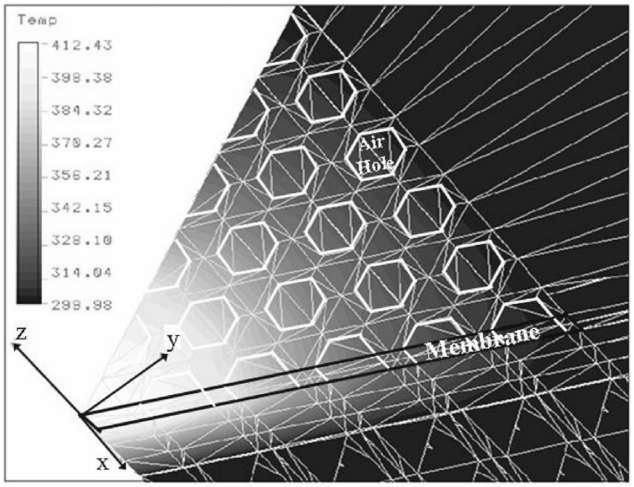

FIG. 2. Heat transfer analysis result of the photonic crystal defect cavity membrane structure optically pumped at 7 mW with 4% duty cycle.

lattice and the z axis is the direction of epitaxial growth. The temperature increase due to optical pumping can be as high as 112 K in the defect region. Thus, we expect the redshift of the gain spectrum to be significant and this is consistent with the fact that we observed lasing at longer wavelength. This result also indicates that the dominant contribution to the increasing temperature of the membrane when the substrate temperature increases from 20 °C to 50 °C is the pump laser beam.

Temperature-dependent measurements are performed on these photonic crystal defect lasers and lasing up to a substrate temperature of 50 °C is obtained. 50 °C is the highest temperature we can obtain with our TEC system, and there is no indication that 50 °C is the highest operating temperature for our photonic crystal lasers. Figure 3 shows a plot of lasing wavelength versus substrate temperature for a typical defect laser with 20 ns pulse width at a repetition rate of 0.5 MHz (1% duty cycle). The thermoelectric temperature controller is used to vary the temperature of the substrate of the sample. In order for the temperature to be uniformly distributed and stabilized at the setting value, at least 15 min are needed. The lasing wavelength increases almost linearly as the substrate temperature increases from 20 °C to 50 °C. The increase in lasing wavelength with increased temperature is approximately 0.5 Å/K. This result is compared with data of

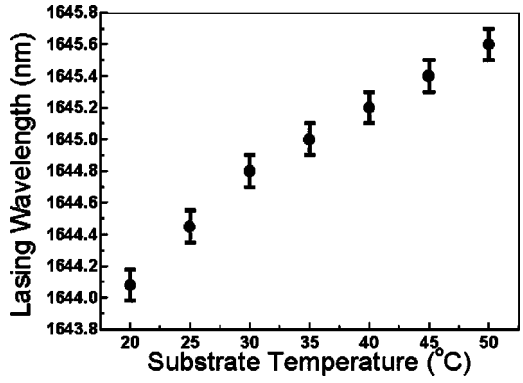

FIG. 3. A plot showing the lasing wavelength versus the substrate temperature. The total increase in wavelength is 1.5 nm when substrate temperature varies from 20 °C to 50 °C.

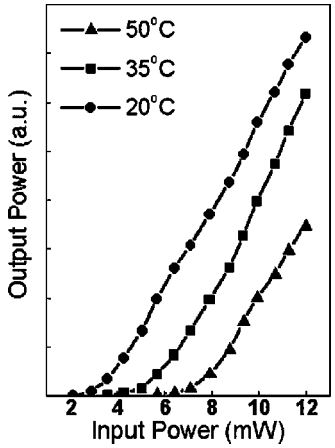

FIG. 4. $L-L$ curves of a typical defect cavity showing the output power at the lasing wavelength versus the incident pump power for temperatures of 20 °C, 35 °C, and 50 °C.

the thermal expansion rate and temperature dependence of refractive index dn/dT of InP, using

$$\frac{d\lambda/dT}{\lambda} = \frac{dL/dT}{L} + \frac{dn/dT}{n}, \tag{1}$$

where λ, T, L, and n represent lasing wavelength, cavity temperature, effective cavity length of the resonant mode, and refractive index, respectively. Using the experimental results for InP, and plugging in the value of thermal expansion ratio 5×10^{-6}/°C,[8] and the temperature coefficient of the refractive index 1×10^{-4}/°C,[9] we obtain a value of 3.5×10^{-5}/°C. This agrees well with $(d\lambda/dT)/\lambda = 3\times10^{-5}$/°C calculated from the experimental results shown in Fig. 3. Hence, the near linear redshift of the lasing wavelength with increasing substrate temperature can be explained by the near linear property of the thermal expansion and the refractive index shift of the semiconductor media in the measured temperature range, and is clearly dominated by the refractive index change. This result also shows the same order of wavelength shift with temperature as distributed feedback (DFB) laser results in the InGaAsP material system.

The temperature characteristic of the threshold pump power of photonic crystal lasers was also investigated. Figure 4 shows the collected light output power versus the incident VCSEL pump power ($L-L$ curve) of a typical defect cavity for substrate temperatures of 20 °C, 35 °C, and 50 °C with 20 ns pulse width at a repetition rate of 0.5 MHz. The threshold input powers are 3.2 mW, 5.3 mW, and 7.4 mW for substrate temperatures 20 °C, 35 °C, and 50 °C, respectively. The threshold pump power increases with the substrate temperature and the characteristic temperature T_o is 37.7 K. It is not clear how to compare these data to that of edge-emitting lasers with the same active region because, as we pointed out, the membrane is much hotter than the substrate temperature, and we expect that there is a significant nonradiative surface recombination component of the threshold pump power. We also note that the measured external efficiencies of the photonic crystal lasers do not decrease monotonically with increasing temperature as observed in InGaAsP edge emitters. This could come from slight differences in the optical alignment of our measurements at three different temperatures, however.

In conclusion, we have demonstrated the operation of photonic crystal lasers for substrate temperatures up to 50 °C. We have also measured the spectral shift in operating wavelength as a function of the operating substrate temperature. These experiments give us an overview of the thermal effects influencing the performance of the photonic crystal membrane defect lasers. It is shown that the effect of substrate temperature on the defect laser wavelength can be explained simply by the temperature dependence of the refractive index alone. The threshold pump power of the photonic crystal membrane laser changes significantly for a 30 °C change of the substrate temperature.

This material is based upon work supported in part by the U. S. Army Research Laboratory and the U. S. Army Research Office under Contract No. DAAD 19-99-1-0121 and in part by the Defense Advanced Research Projects Agency under Contract Nos. MDA972-00-1-0019 and N00014-00-c-8079.

[1] O. J. Painter, R. K. Lee, A. Scherer, A. Yariv, J. D. O'Brien, P. D. Dapkus, and I. Kim, Science **284**, 1819 (1999).
[2] O. J. Painter, A. Husain, A. Scherer, J. D. O'Brien, I. Kim, and P. D. Dapkus, J. Lightwave Technol. **17**, 2082 (1999).
[3] J. K. Hwang, H. Y. Ryu, D. S. Song, I. Y. Han, H. W. Song, H. K. Park, and Y. H. Lee, Appl. Phys. Lett. **76**, 2982 (2000).
[4] P.-T. Lee, J. R. Cao, S.-J. Choi, Z.-J. Wei, J. D. O'Brien, and P. D. Dapkus, IEEE Photonics Technol. Lett. **14**, 435 (2002).
[5] C. Monat, C. Seassal, X. Letartre, P. Viktorovitch, P. Regreny, M. Gendry, P. Rojo-Romeo, G. Hollinger, E. Jalaguier, S. Pocas, and B. Aspar, IEEE Electron Lett. **37**, 764 (2001).
[6] J. K. Hwang, H. Y. Ryu, D. S. Song, I. Y. Han, H. K. Park, D. H. Jang, and Y. H. Lee, IEEE Photonics Technol. Lett. **12**, 1295 (2000).
[7] J. R. Cao, P.-T. Lee, S.-J. Choi, R. Shafiiha, S.-J. Choi, J. D. O'Brien, and P. D. Dapkus, J. Vac. Sci. Technol. B **20**, 618 (2002).
[8] R. Bisaro, P. Merenda, and T. P. Pearsall, Appl. Phys. Lett. **34**, 100 (1979).
[9] V. B. Bogdanov, V. T. Prokopenko, and A. D. Yaskov, Opt. Spectrosc. USSR **60**, 68 (1986).